

## H3 relaxin mediated neuroprotection in Alzheimer's disease pathology induced by streptozotocin in mouse models: Impact on memory improvement, autophagy and PI3K/Akt-mTOR signalling pathway

HUIYU ZHAO<sup>1</sup>  
YUHONG SUN<sup>2</sup>  
SHAIK ALTHAF HUSSAIN<sup>3</sup>  
HUA GAO<sup>4\*</sup> 

<sup>1</sup> Department of Neurology  
Harbin 242 Hospital, Harbin  
150066, China

<sup>2</sup> Department of Regular Physical  
Examination Center, Shandong  
Public Health Clinical Center  
Shandong University, Jinan  
250100, China

<sup>3</sup> Department of Zoology, College  
of Science, King Saud University  
P.O. Box 2454, Riyadh 11451  
Saudi Arabia

<sup>4</sup> Department of Neurology  
Shaanxi Aerospace Hospital  
Xi'an, 710038, China

### ABSTRACT

Alzheimer's disease (AD) is characterised by  $\beta$ -amyloid ( $A\beta$ ) plaque accumulation and tau hyperphosphorylation. H3 relaxin, a neuropeptide, is known to exert neuroprotective effects. In this study, we investigated how H3 relaxin confers neuroprotection in a streptozotocin (STZ)-induced mouse model and modulates PI3K/Akt-mTOR signalling. Mice were divided into four groups ( $n = 6$  per group): control (saline), STZ, STZ + H3 relaxin, and STZ + donepezil. Following STZ induction, H3 relaxin (1  $\mu$ g per day) was administered intracerebroventricularly (ICV) for 14 consecutive days, whereas donepezil (2.5 mg  $kg^{-1}$  per day) was administered orally for the same duration. Cognitive performance was assessed using the Morris water maze (MWM) test.  $A\beta$  deposition in the cortex was evaluated through immunohistochemistry. Western blotting was conducted for tau phosphorylation, PI3K/Akt/mTOR signalling, and autophagy markers in the hippocampus. Oxidative stress and inflammation markers were measured using ELISA. H3 relaxin markedly improved memory by decreasing escape latency and duration while spending more time in the target quadrant in the MWM test. Additionally, H3 relaxin reduced  $A\beta$  plaque burden and tau phosphorylation (Ser396/404) while enhancing PI3K/Akt-mTOR signalling. Oxidative stress was attenuated, as evidenced by increased GSH and HO-1 levels and reduced MDA and  $H_2O_2$  concentrations. Moreover, markers of inflammation, NF- $\kappa$ B and TNF- $\alpha$  were suppressed. Overall, H3 relaxin ameliorated cognitive deficits in STZ-induced AD mice through modulation of impaired PI3K/Akt-mTOR signalling, reduction of  $A\beta$  and tau pathology, and promotion of autophagy.

**Keywords:** Alzheimer's disease, streptozotocin, H3 relaxin, neuroprotection, memory improvement

Accepted March 6, 2026  
Published online March 7, 2026

### INTRODUCTION

Alzheimer's disease (AD) is the most common neurodegenerative disorder and involves a gradual decline in cognitive skills, progressive amnesia, and changes in behaviour

\* Correspondence; e-mail: g\_hua2003@outlook.com

(1). Due to global improvements in healthcare systems and life expectancy, there is a rapidly rising elderly population, which in turn increases the projected prevalence of AD (2). Report estimates that by 2025, there will be 7.2 million Americans older than 65 years suffering from AD, inducing a higher mortality rate than breast and prostate cancer combined (3).

The pathogenesis of AD is not fully understood (4). It is said to result from a combination of factors: the build-up of amyloid-beta ( $A\beta$ ) plaques, the development of senile neurofibrillary tangles (NFTs) from tau protein hyperphosphorylation, inflammation in the brain, oxidative stress and disruption of synaptic function (5). Important molecular components of AD are the alterations in the signalling of the PI3K/Akt-mTOR pathway, as this influences the rate of neuronal death, metabolism, and synaptic activity (6). The activation of PI3K leads to downstream inhibitory activity on GSK-3 $\beta$ , thereby reducing the production and hyperphosphorylation of tau protein (7). On the other hand, the dysregulation of this pathway, particularly due to excessive mTOR activity, worsens tau pathology by failing to clear tau proteins through autophagy and accelerating neurodegeneration (8). The intracellular degradation process of autophagy is extremely important because it helps in maintaining equilibrium in the neurons by removing damaged organelles and aggregates of proteins (9). Initially in AD, there is a protective mechanism provided by autophagy (10). Unfortunately, in the course of the disease, autophagic flux becomes impaired (11). The markers typically used to track the steps of the autophagy process are LC3 and the other known markers are ATG5 and beclin 1, which are classified under autophagy-associated proteins (12). The conversion of LC3-I to LC3-II (lipidated version) is considered an indicator of autophagosome formation and determines the rates of autophagy, and therefore, this process is extensively investigated nowadays (13). Key contributors to the formation and working of the autophagic machine are ATG5, which is essential for the elongation of autophagosomes, and beclin 1, which initiates the nucleation of the autophagosomes (14). These proteins have shown decreased levels, which have been correlated with deficient autophagy and elevated levels of  $A\beta$  in AD animal and cellular models (15).

H3 relaxin or insulin-like peptide-7 (INSL7) is a neuropeptide of the insulin/relaxin family that is believed to modulate stress, feeding, and higher-order functions, including cognition (16). It is mainly produced by the neurons of the nucleus incertus (NI) in the brainstem and acts through its RXFP3 receptor, which is abundantly expressed in brain regions pivotal for emotion, memory, and arousal, such as the limbic system, hypothalamus, thalamus, and neocortex (17). H3 relaxin can also interact with RXFP1, although this receptor is better known for its functions mediated through relaxin-2 (18). Importantly, RXFP3 signalling has also been correlated with stress, anxiety, and depression-related behaviours, where pharmacological modulation in the form of activation tends to lead to anxiolytic and antidepressant-like effects in rodent models (16).

Based on the literature, there is limited information on the role of H3 relaxin and its receptors in the context of neurodegenerative diseases such as AD (19). Conflicting evidence suggests that RXFP1 and RXFP3 are expressed in brain regions that are known to be affected in AD; however, whether their expression or function in the context of the disease is altered remains unknown (17). The role of H3 relaxin signalling in neurodegeneration, particularly its regulation of autophagy and the PI3K/Akt-mTOR signalling pathway, is an area where novel neuroprotective mechanisms may be explored.

This study focused on the therapeutic effects of H3 relaxin within the context of streptozotocin (STZ) induced AD neurodegenerative changes in mouse models. We evaluated cognitive capabilities, alterations in autophagy-related markers, and changes in the PI3K/Akt-mTOR signalling pathway. We aim to clarify the possible role of H3 relaxin in ameliorating Alzheimer's pathology in the context of neuroprotection against memory loss.

## EXPERIMENTAL

### *Animals*

For this current experimental study, we used male Swiss Albino mice aged 8 weeks old and weighing 20–30 grams purchased from Guoruiyinu Co., Ltd., China. The mice were kept under laboratory conditions where they could freely access food and water, with a temperature maintained at  $25 \pm 5$  °C. Lights were on for 12 hours each day. Before starting the experiments, the animals underwent a two-week period of acclimatisation. To reduce confounding effects related to circadian rhythms, all tests were conducted daily at the same time.

The study protocol was approved by the ethical committee of the Shaanxi Aerospace Hospital, Xi'an, China (SAH/23.2022). All animals were treated humanely, with efforts made to minimise discomfort and suffering throughout the study.

### *Drugs*

Donepezil and streptozotocin were obtained from Sigma-Aldrich, USA. Synthetic H3 relaxin was obtained from Phoenix Pharmaceuticals, USA (Cat# 035-36) as a lyophilised powder. The peptide was reconstituted in sterile distilled water to prepare a stock solution, aliquoted to avoid repeated freeze-thaw cycles, and stored at  $-20$  °C. Working solutions were freshly prepared prior to administration.

### *Induction of Alzheimer's disease*

Alzheimer's disease was induced through intracerebroventricular (ICV) injection of STZ by following the freehand technique (20). A concentration of  $3 \text{ mg kg}^{-1}$  STZ (dissolved in 0.9 % sterile saline) was given to the mice. The mice were anaesthetised through intraperitoneal (*i.p.*) injections of xylazine ( $10 \text{ mg kg}^{-1}$ ) and ketamine ( $80 \text{ mg kg}^{-1}$ ) (21). The technique involves holding the head of the mouse by applying downward force over the ears. The bregma can be found by sighting an equilateral triangle made by the two eyes and the mid-point of the skull. The needle was thus inserted about 1 mm lateral to this point and advanced through the skin and skull. It was noted that mice resumed normal behavior after STZ injection within an average of 1 minute.

### *Experimental design*

The animals were randomly divided into four groups of six animals each. Group 1 (control) received an ICV injection of  $3 \mu\text{L}$  0.9 % sterile saline. Groups 2, 3, and 4 received two ICV injections of STZ ( $3 \text{ mg kg}^{-1}$  in  $3 \mu\text{L}$  0.9 % sterile saline) on day 1 and day 3 to

induce an Alzheimer's-like cognitive impairment model. Group 2 served as the STZ-only group, while Groups 3 and 4 received post-STZ treatment. Group 3 received synthetic H3 relaxin administered intracerebroventricularly at a dose of  $1 \mu\text{g kg}^{-1}$  per day for 14 consecutive days, spanning the final two weeks prior to the experiment's conclusion. Group 4 received donepezil administered orally at a dose of  $2.5 \text{ mg kg}^{-1}$  per day for the same 14 consecutive days, following STZ induction. Thus, both H3 relaxin and donepezil were administered for 14 days (2 weeks). During this treatment period, mice in the STZ-only and control groups received the corresponding vehicle in the same schedule. Behavioural assessments were conducted using the MWM probe test and object recognition tests 24 hours after the last dose of treatment, with care taken to minimise circadian variability in behavior pre- and post-testing. After behaviour testing was completed, the groups were split into two sets ( $n = 6$ ) each. Mice were euthanised through an overdose of thiopental ( $200 \text{ mg kg}^{-1}$ , intraperitoneally), without transcardial perfusion and ICV injection accuracy was confirmed *via* visual inspection, and brains were excised immediately. The animals were then divided into two sets. Whole brains of one set were preserved in 10 % formalin-saline for immunohistochemical analysis. Brains from the second set were divided into two hemispheres; left hemispheres were used for biochemical analysis by Western blot, while right hemispheres were used for ELISA studies.

#### *Morris water maze test (MWM)*

The MWM features a round pool made of stainless steel (150-cm diameter, 60-cm height) filled with water to a depth of 30 cm and maintained at room temperature. The pool was split into four quadrants (NW, NE, SE, SW) by two crossing threads attached to the rim, which were labelled as north (N), south (S), east (E) and west (W). There was a submerged wooden platform (10 cm wide, 28 cm high) painted black, placed 2 cm beneath the water surface at the centre of one quadrant. It was made invisible by non-toxic powdered skim milk, which was used to opacify the water. Control mice were able to learn the location of the platform quickly. The test lasted 5 successive days. Each day from 1–4, each mouse participated in two consecutive trials with fifteen-minute breaks in between. Mice who found the platform within two minutes stayed on it for 20 seconds, while those who couldn't find it were assisted to the platform and allowed twenty seconds of rest.

Mean escape latency (MEL), which is the time required to find the platform, was recorded over the four-day acquisition phase (22). Subsequently, on day five, a probe test was conducted where the platform was removed to test recall by allowing each mouse to explore the arena for 60 seconds. The duration spent in the target quadrant was recorded.

#### *Object recognition test*

The object recognition test was done in a wooden box measuring ( $30 \times 30 \times 30 \text{ cm}$ ) for 3 days straight. Day 1 (habituation) involved a 10-minute exploration of the empty box. Day 2 was dedicated to familiarisation. Mice were allowed to explore the box with two identical objects (of the same size, shape, and colour) placed in the far corners for 10 minutes. During the third day (test phase), mice were given 5 minutes to explore the box where one of the previous objects had been replaced with an entirely different one. All features of this object were novel. The box and objects were cleaned with 70 % ethanol between trials in order to

remove odour cues. Cognitive function was assessed via the recognition index (time spent exploring the novel object divided by total time spent exploring the two objects) and the discrimination index (DI) (difference between time spent exploring novel and familiar objects divided by the total time spent), with values ranging between -1 and +1. A positive DI indicates preference towards the newer object, while a negative DI means preference towards the previously familiar object, and zero indicates no particular preference.

### *Western blot analysis*

Tissues were lysed in RIPA buffer. It was followed by centrifugation at  $16,000 \times g$  for 30 minutes at  $4^\circ\text{C}$ . The supernatant was then collected, and protein concentration was measured using the Bradford assay. After tissue lysis,  $20\ \mu\text{g}$  of proteins was isolated and resolved on 8–10 % SDS-PAGE. Subsequently, proteins were transferred to PVDF membranes and blocked with 3 % BSA in Tween-TBS. It was followed by washing and subsequent incubation with the primary antibody. The primary antibodies used were anti-PI3K (Cell Signaling Technology, The Netherlands, Cat.# 4292, 1:1000), anti-p-PI3K p85 (Tyr458) (Cell Signaling Technology, Cat.# 4228L, 1:1000), anti-Akt (Abcam, UK, Cat.# ab8805, 1:1000), anti-p-Akt (Ser473) (Thermo Fisher Scientific, USA, Cat.# 200-301-B19, 1:1000), anti-mTOR (Cell Signaling Technology, Cat.# 2972, 1:1000), anti-p-mTOR (Ser2448) (Cell Signaling Technology, Cat.# 2971, 1:1000), anti-tau (Ser396) (Abcam, Cat.# ab109390, 1:1000), anti-tau (Ser404) (Thermo Fisher Scientific, Cat.# 44-758G, 1:1000), anti-beclin 1 (Cell Signaling Technology, Cat.# 4122, 1:1000), anti-LC3-I/II (Novus Biologicals, USA, Cat.# NB100-2331, 1:250), anti-ATG5 (Novus Biologicals, Ca.t# NBP1-49751, 1:1000), and anti- $\beta$ -actin (Sigma-Aldrich, USA, Cat.# A5316, 1:1000).

Membranes were treated for 1 hour with HRP-conjugated anti-rabbit (Cell Signaling Technology, Cat.# 7074, 1:5000) or anti-mouse (Cell Signaling Technology, Cat.# 7076, 1:5000) secondary antibodies, followed by Clarity<sup>TM</sup> Western ECL substrate detection (Bio-Rad, USA, Cat.# 1705060) and densitometric analysis relative to  $\beta$ -actin using a Bio-Rad Gel Doc<sup>TM</sup> imaging system. Blots were performed using hippocampal/cortical lysates from  $n = 6$  mice per group, and each experiment was repeated three times.

### *Immunohistochemistry research*

Formalin-fixed, paraffin-embedded brain sections ( $8\ \mu\text{m}$  thick) were stained for  $\beta$ -amyloid ( $\text{A}\beta$ ) using anti- $\text{A}\beta$  antibody (clone 6E10, recognises  $\text{A}\beta$ 1-16; mouse monoclonal, Abcam, Cat.# ab2539, 1:500 dilution). Immunoreactivity was analysed in the frontal cortex (cerebral cortex). In this case, section dewaxing was conducted first, followed by antigen retrieval using microwave ovens in 3 % hydrogen peroxide solution. Primary antibody incubation was performed using 0.1 % Tween 20/Tris Buffered Saline (TBS) and 5 % non-fat dry milk for 15 hours at room temperature. As part of controlling nonspecific staining, a sample devoid of primary antibodies was introduced. HRP-labelled secondary antibodies were applied for 1 hour, followed by detection using diaminobenzidine and counterstaining with hematoxylin. Immunohistochemical scoring of  $\text{A}\beta$  plaques was performed semi-quantitatively: 0 (no staining), 1+ (0 to 10 plaques), 2+ (greater than 10 dispersed plaques), 3+ (staining of most cortex) or 4+ (staining of cortex approaching confluent) (23). Quantification was achieved through the use of ImageJ (v1.46a, NIH, USA) for three random fields of view on each section.

## ELISA

Following isolation of the left cerebral hemispheres, hippocampal samples were carefully dissected under a stereomicroscope using anatomical landmarks and sliced on an ice-salt mixture to prevent protein degradation, maintaining proteins for further analyses. The tissues were then weighed and homogenised in phosphate-buffered saline (PBS, pH 7.4) supplemented with a protease inhibitor cocktail to achieve a 10 % (*m/V*) tissue homogenate. After homogenising, samples were subjected to high-speed centrifugation at 12,000 × *g* for 15 min at 4 °C to remove cellular debris. Clear supernatants were collected, aliquoted, and stored at -80 °C until further analysis.

Total protein concentration in each sample was determined using a bicinchoninic acid (BCA) protein assay, and ELISA results were normalised to protein content (per mg protein). Using specific ELISA kits, the levels of various important oxidative stress markers GSH (Cayman Chemical, USA, Cat.# 703002), HO-1 (Abcam, Cat.# ab207093), MDA (Sigma-Aldrich, Cat.# MAK085), and H<sub>2</sub>O<sub>2</sub> (Abcam, Cat.# ab102500) and inflammatory mediators TNF- $\alpha$  (R&D Systems, Cat.# MTA00B) and NF- $\kappa$ B (Abcam, Cat.# ab176648), were quantitatively assessed in triplicates according to the manufacturer's instructions. Absorbance was measured using a microplate spectrophotometer (BioTek Synergy™ HTX, Agilent Technologies, USA), and concentrations were calculated from assay-specific standard curves.

## Statistical analysis

Data are expressed as mean  $\pm$  SEM. Statistical analysis was performed using GraphPad Prism (v7, GraphPad Software Inc, USA). Comparisons among multiple groups were carried out using one-way ANOVA followed by Tukey's multiple comparison test. The Kolmogorov-Smirnov test was used to assess normality, and Bartlett's test assessed the homogeneity of variance. The ROUT test was used to identify outliers. The value of  $p < 0.05$  was considered statistically significant.

## RESULTS AND DISCUSSION

### *Effects of H3 relaxin on animal behaviour and cognitive function in the novel object recognition test*

Memory impairment is a well-established diagnostic criterion of AD (24), and it was also conspicuously evident in our STZ model, as demonstrated by increased MELs and reduced time spent in the target quadrant during the MWM test, along with impaired object recognition performance. Administration of H3 relaxin led to a remarkable improvement in cognitive functions, which was indicated by a decrease in escape latency and an increase in spatial memory retention at comparable levels to donepezil, a quintessential drug for managing AD symptoms. These findings strongly suggest that H3 relaxin can reverse STZ-induced memory deficits.

MWM test was carried out to evaluate the spatial learning and the memory of animals that underwent STZ administration, with comparison to both control and donepezil-treated groups, to gauge the impact of H3 relaxin. Throughout the study, the animals

underwent marked changes in behavior, particularly in relation to locating the hidden platform. During the first three days post-STZ injection, animals showed a steady decline in the time taken to reach the platform, suggesting a degree of learning, although the STZ-treated group showed the highest MEL. Overall, compared to the control group, STZ-treated animals navigated the space with the greatest impairment.

During the second, third, and fourth trial days, STZ-treated mice showed notable increases in latency compared to control cohorts, demonstrating the cognitive impact of STZ. However, there was no significant difference between the groups when treated with either H3 relaxin or donepezil, as there was significant reduction in MEL without apparent differences across groups. This suggests that both H3 relaxin and donepezil improve STZ-induced spatial learning deficits, although a direct comparison between the two treatments was not performed.

On the day of the test when the platform was taken out to assess the memories of the control animals, the STZ group had a distinctly lower amount of time spent at the target quadrant, suggesting impaired memory retention. Treating them with either H3 relaxin or donepezil ameliorated this deficit, with treated animals spending a greater amount of time in the target quadrant compared to the untreated STZ group, without significant differences between the two treatments. Collectively, these observations indicate that H3 relaxin administered to STZ-treated mice significantly improved spatial memory retention, achieving effects that were indistinguishable from those observed in the donepezil-treated group (Fig. 1a,b).

To further evaluate cognitive and memory deficits caused by STZ, the novel object recognition test was performed with emphasis on the effects of H3 relaxin. This test measures an animal's capability to recognise the difference between new objects and those that have been previously encountered, in order to demonstrate recognition memory (25). STZ-treated animals had a much lower preference towards the novel object, and this was shown by a decrease in the time spent exploring the object relative to control animals, confirming significant memory impairment. Treatment with H3 relaxin substantially restored memory and increased the time spent exploring the novel object compared to the STZ group.

Also, STZ-injected mice demonstrated a reduction in the discrimination index, calculated by the difference in time spent on novel and familiar objects, relative to the controls. H3 relaxin treatment improved this discrimination deficit, for the novel object compared to the STZ group. These findings underscore the potency of both compounds in offsetting the STZ-induced recognition memory deficits with no significant difference between H3 relaxin and donepezil in their restorative efficacy (Fig. 1c,d).

### *H3 relaxin effects on amyloid plaque deposition and tau hyperphosphorylation*

Accumulation of A $\beta$  plaques and hyperphosphorylated tau are two hallmarks of AD pathology (26). The reduction of A $\beta$  plaques and tau phosphorylation at Ser396/Ser404 observed after H3 relaxin treatment illustrates the characteristic signature of its effects on these hallmark neuropathological features of AD. Although donepezil treatment demonstrated slightly greater clearance of A $\beta$  plaques compared to the H3 relaxin group, H3 relaxin treatment still produced a significant reduction in A $\beta$  plaques, supporting its potential disease-modifying effects (27). These results may stem from changes in autophagy modulation and PI3K/Akt/mTOR signalling as both pathways are essential for the homeostasis of cellular proteins and tau metabolism (28).

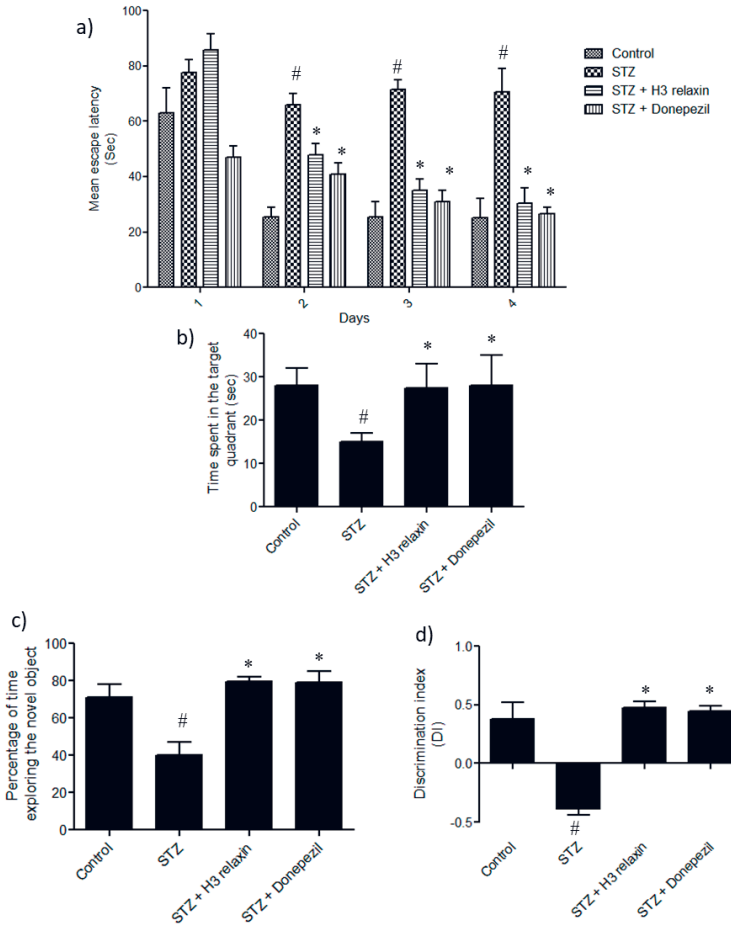


Fig. 1. a) Mean escape latency (MEL), time needed to find the hidden platform during the training trials; b) time spent exploring the target quadrant in the probe trial was taken as an indicator for memory retention after the platform was removed; c) time spent on the novel object relates to activity aimed at recognizing something new; d) the discrimination index was calculated as the difference in time spent interacting with the novel object versus the familiar one, which indicates recognition memory capacity. Each experiment included biological replicates ( $n = 6$ ) and was performed in triplicate. #  $p < 0.05$ , vs. control group, and \*  $p < 0.05$ , vs. STZ group.

As expected, the control group showed no signs of amyloid plaque deposition in the brain slices they analysed. However, the STZ-treated group showed significant amyloid accumulation, indicating the development of neurodegenerative pathology. This effect is associated with impaired brain insulin signalling, leading to dysregulation of the PI3K/Akt/mTOR pathway, activation of GSK-3 $\beta$ , increased amyloidogenic amyloid precursor protein (APP) processing, reduced A $\beta$  clearance *via* insulin-degrading enzyme (IDE), and enhanced neuroinflammation through the AGE/RAGE/NF- $\kappa$ B pathway, as reported in

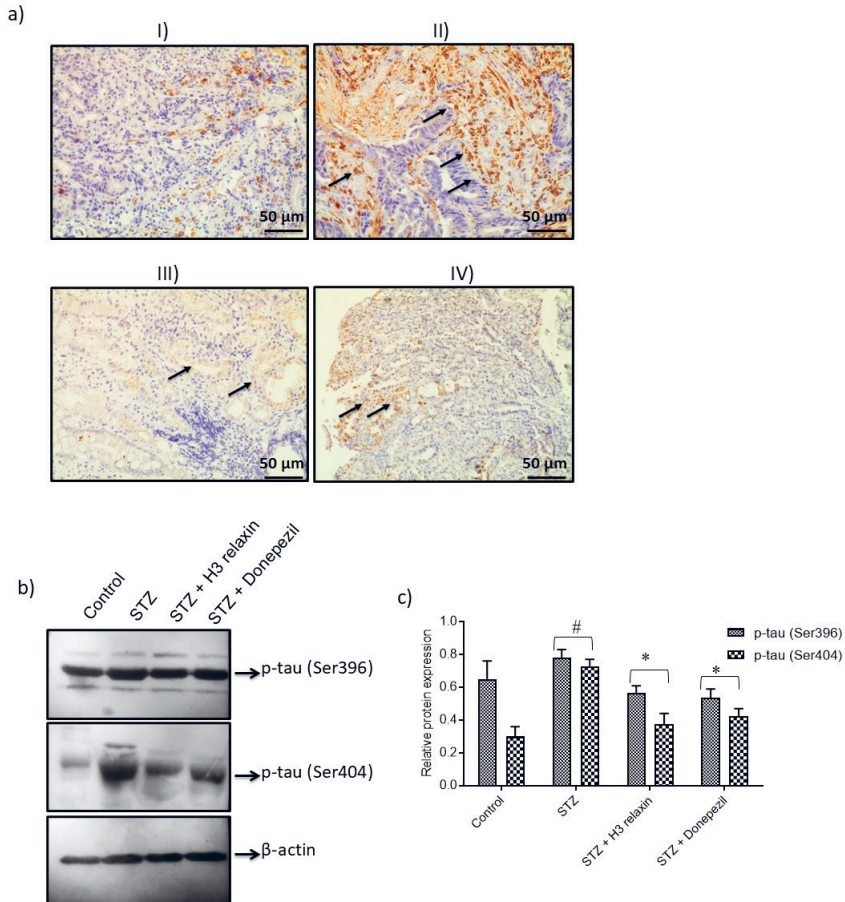


Fig. 2. Effect of H3 relaxin on frontal cortical histopathology and p-tau expression in STZ-induced Alzheimer-like mice. a) Photomicrographs of the frontal cortex of mice after STZ administration and treatment with H3 relaxin. (I) Cortex of control mice showing normal histological architecture of the brain. (II) Cortex of STZ-treated mice shows extensive neuronal degeneration and prominent amyloid plaque deposition (arrowhead). (III) Cortex of STZ + H3 relaxin-treated mice demonstrates restored histological architecture with reduced neuronal loss and mild amyloid plaque deposition (arrowhead). (IV) The cortex of donepezil-treated mice displays near normal histological structure with sparse amyloid plaques. Sections were stained with hematoxylin and eosin (H&E) and images captured at 40× magnification. Scale bar = 50 μm; b) expression levels of p-tau (Ser 396/404) assessed by Western blotting; c) densitometry analysis of the Western blot was performed using ImageJ. Protein levels were normalized to β-actin, and data are presented as mean ± SEM. Each experiment included biological replicates ( $n = 6$ ) and was performed in triplicate. # $p < 0.05$ , vs. control group, and \* $p < 0.05$ , vs. STZ group.

STZ-induced and transgenic AD models (29). H3 relaxin treatment decreased the number and size of amyloid plaques, while donepezil treatment almost completely removed the plaques in most of the regions examined. These results clearly reveal that H3 relaxin

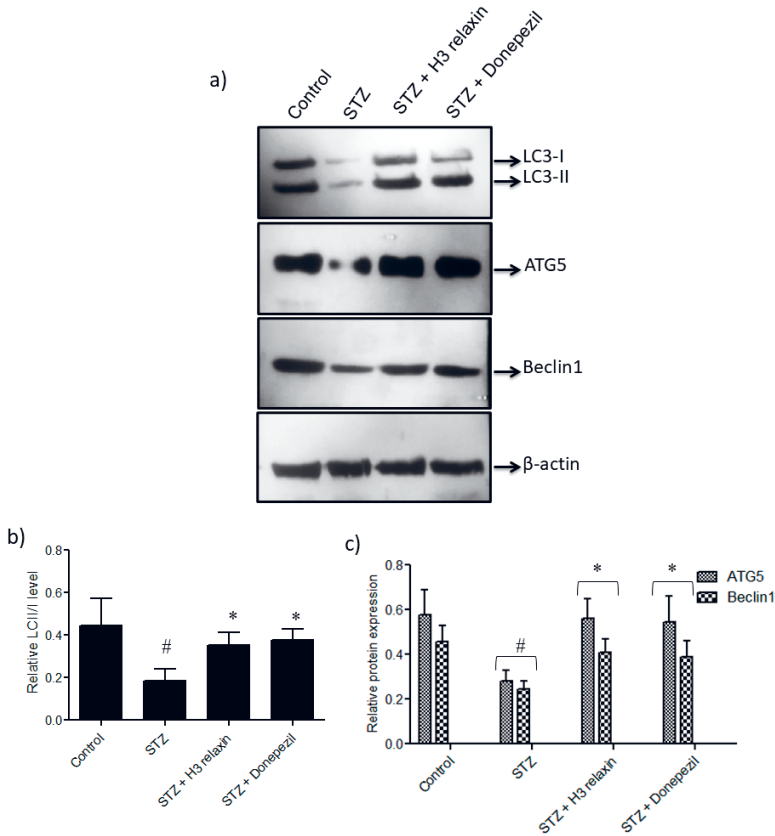


Fig. 3. H3 relaxin upregulates autophagy-related protein expression in STZ-induced Alzheimer-like mice. a) Western blot analysis showing the protein expression of LC3-II, LC3-I, ATG5, and beclin 1; b) and c) densitometry analysis of the blots was performed using ImageJ. Protein expression was normalised to  $\beta$ -actin. Each experiment included biological replicates ( $n = 6$ ) and was performed in triplicate. # $p < 0.05$ , vs. control group, and \* $p < 0.05$ , vs. STZ group.

effectively reduced amyloid burden, with effects that closely resembled those of donepezil (Fig. 2a).

The AD model with STZ showed distinct protein expression changes within the hippocampus that are associated with neurodegeneration. More specifically, tau protein was hyperphosphorylated, demonstrating an Alzheimer's-like pathology and markedly increased levels compared to control groups; however, H3 relaxin treatment significantly lowered the hyperphosphorylation of tau protein (Fig. 2b,c).

#### *Influence of H3 relaxin on expressions of autophagy-related proteins*

Autophagic processes are essential for the degradation of aggregated proteins such as  $A\beta$  and hyperphosphorylated tau (30). STZ has been shown to impair autophagic flux with

decreased ratios of LC3-II/LC3-I, along with reduced expression levels of beclin 1 and ATG5. These findings are consistent with reports of defective autophagy in AD, which contributes to the accumulation of neurotoxic proteins (31, 32). H3 relaxin treatment restored these markers of autophagy-related markers, suggesting enhanced formation of autophagosomes and improved autophagic degradation. Considering the interplay between PI3K/Akt/mTOR signalling and autophagy, it is reasonable to suggest that H3 relaxin restored autophagy through modulation of these signalling pathways. These results highlight H3 relaxin as a possible candidate for modulating cellular proteostasis and slowing neurodegenerative progression.

To understand the extent of the modulatory effect of H3 relaxin on autophagy, we assessed the levels of prominent autophagy proteins, namely LC3, ATG5, and beclin 1, using Western blot analysis. The STZ murine model exhibited a significant decrease in the ratio of LC3-II to LC3-I (LC3-II/I) as well as the relative expression levels of ATG5 and beclin 1, when compared to the control group (Fig. 3). This suggests that the STZ group demonstrated suppressed autophagic activity.

As noted, H3 relaxin treatment restored the level of expression of proteins involved in autophagy. The ratio of LC3-II to LC3-I (LC3-II/I), a widely accepted marker of autophagosome formation, was enhanced in the H3 relaxin-treated group compared to the STZ group, demonstrating enhanced maturation and accumulation of autophagosomes. In addition, the levels of ATG5, a crucial component in the elongation of autophagosomes, and beclin 1, an essential pro-autophagic factor that begins the nucleation of autophagosomes, were shown to markedly increase with treatment of H3 relaxin. These findings imply that H3 relaxin mitigates the STZ induced slowdown of autophagy in STZ-treated mice, in effect restoring the autophagic process and supporting cellular metabolic homeostasis under pathological conditions.

### *The impacts of H3 relaxin on oxidative stress markers and neuroinflammation*

STZ-treated mice displayed elevated levels of MDA and H<sub>2</sub>O<sub>2</sub> while showing low amounts of antioxidants such as HO-1 and GSH. This observation reflects impaired synaptic and neuronal redox capacity. In regard to redox balance, administration of H3 relaxin significantly enhanced antioxidant defences and limited lipid peroxidation. Such an antioxidant effect could support the neuroprotection observed previously since diminished oxidative stress is known to improve synaptic function and enhance cognitive performance in AD models (33).

Neuroinflammation, which is associated with AD, is understood to exacerbate amyloid- and tau-related pathologies (34). In the context of the disease model, it was noticed that the exogenous administration of STZ led to an increase in TNF- $\alpha$  and NF- $\kappa$ B, both of which are indicative of an inflammatory response. Given the well-established reciprocal regulation between NF- $\kappa$ B and the antioxidant transcription factor Nrf2, this heightened inflammatory state may indirectly reflect an impairment of Nrf2-mediated cytoprotective signalling, which has been widely reported in STZ-induced Alzheimer's disease models. Furthermore, treatment with H3 relaxin markedly suppressed these inflammatory markers, alongside donepezil, indicating a robust anti-inflammatory effect. These results are consistent with previous findings that demonstrated RXFP3 activation, the receptor medi-

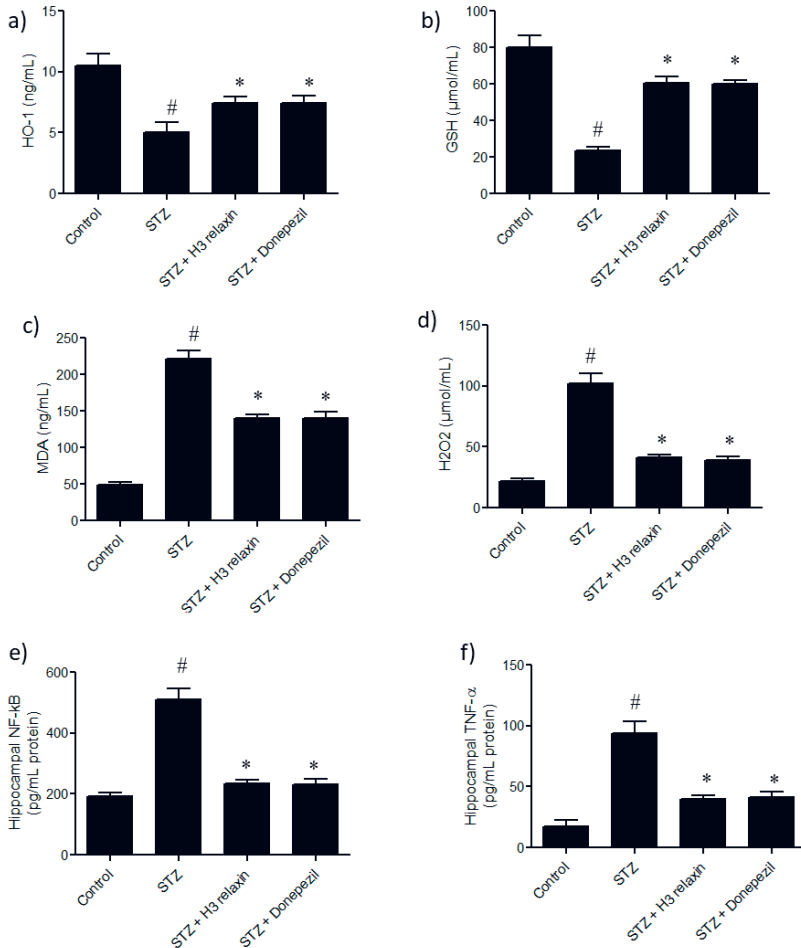


Fig. 4. Impact of H3 relaxin on different markers of oxidative stress and neuroinflammatory markers in the brain. a) Concentration of MDA, a by-product of lipid necrosis inflammatory processes; b) amount of H<sub>2</sub>O<sub>2</sub>, assessing the oxidative load; c) amount of GSH, an indicator of the potential to donate electrons; d) content of HO-1, an antioxidant due to its high catalytic activity. The levels of TNF- $\alpha$  (E) and NF- $\kappa\text{B}$  (F) were determined. Each experiment included biological replicates ( $n = 6$ ) and was performed in triplicate. # $p < 0.05$ , vs. control group, and \* $p < 0.05$ , vs. STZ group.

ated by H3 relaxin, leads to reduced inflammation and anxiety-like behaviour (35). Thus, the reduction of neuroinflammatory processes is likely to be a key contributor to the observed improvements in memory and neuropathology in this model.

The STZ treatment resulted in pronounced oxidative stress in the brain relative to its control group, indicated by an imbalance in oxidative stress biomarkers. In particular, STZ-treated animals showed reduced levels of heme oxygenase-1 (HO-1) and decreased glutathione (GSH), which are important cellular antioxidants. Concurrently, elevated

levels of MDA, an indicator of lipid peroxidation, and hydrogen peroxide (H<sub>2</sub>O<sub>2</sub>), a marker of oxidative stress, were observed.

Both H3 relaxin and donepezil treatments were effective in reversing STZ-induced alterations. In both cases, there was an increase in GSH and HO-1 levels, accompanied by reduced MDA and H<sub>2</sub>O<sub>2</sub> concentrations. These findings demonstrate that H3 relaxin and donepezil exert comparable efficacy in mitigating oxidative stress (Fig. 4a–d).

Neuroinflammation was measured as one of the consequences of STZ-induced neurodegeneration by monitoring key pro-inflammatory mediators. Mice injected with STZ exhibited a marked upregulation of NF- $\kappa$ B and increased TNF- $\alpha$  concentrations in brain tissue. The physiological imbalances further point towards the amplification of an inflammatory response.

Administration of H3 relaxin or donepezil significantly attenuated neuroinflammatory markers in STZ-treated mice. Both treatments reduced TNF- $\alpha$  and NF- $\kappa$ B levels, thereby suppressing STZ-induced inflammation. The observed effects following H3 relaxin and donepezil treatment indicate that both agents possess anti-inflammatory activity of comparable magnitude (Fig. 4e,f).

#### *The impact of H3 relaxin on the PI3K/Akt/mTOR pathway*

The dysregulation of the PI3K/Akt/mTOR pathway profoundly affects cell survival, synaptic plasticity, and regulates tau phosphorylation as well as autophagy activity (36). STZ administration is reported to downregulate the phosphorylation of PI3K, Akt, and mTOR, which was consistent with the AD model's suppressed pro-survival signalling environment (37, 38). Treating the AD model with H3 relaxin showed a restoration of phosphorylation levels for these proteins, suggesting that the pathway is reactivated. This is of particular importance since PI3K activation also corresponds with the blockade of GSK-3 $\beta$ , one of the key players in tau hyperphosphorylation, while proper mTOR regulation facilitates the maintenance of balanced autophagic flux (39). These findings are in agreement with other studies showing that reinforcement of the PI3K/Akt pathway improves tau pathology and neurodegeneration in AD models (40).

The STZ-induced AD model in mice is characterised by distinct molecular changes in the hippocampus, a region highly susceptible to AD-related changes. As part of this remodelling, a marked reduction in the phosphorylation status of key signalling proteins within the PI3K/Akt/mTOR pathway was noted. In particular, STZ treatment resulted in a significant reduction in the level of phosphorylated forms of the proteins: p-PI3K, p-Akt and p-mTOR, while there was no significant change in the total amounts of the proteins PI3K, Akt, and mTOR. This decrease in the ratio of phospho-proteins to total proteins suggests impairment of the PI3K/Akt/mTOR signalling pathway, which is critical in neuronal death slowing, synaptic integration, and autophagy regulation, all of which are impaired in AD.

Equally important, treatment with H3 relaxin resulted in a significant increase in levels of the phosphorylated forms of PI3K, Akt, and mTOR compared to the STZ-treated group, indicating a restoration of pathway activity (Fig. 5). These results imply that H3 relaxin may exert a modulatory effect on STZ-induced neurodegenerative processes, potentially mediated through activation of the PI3K/Akt/mTOR signalling axis.

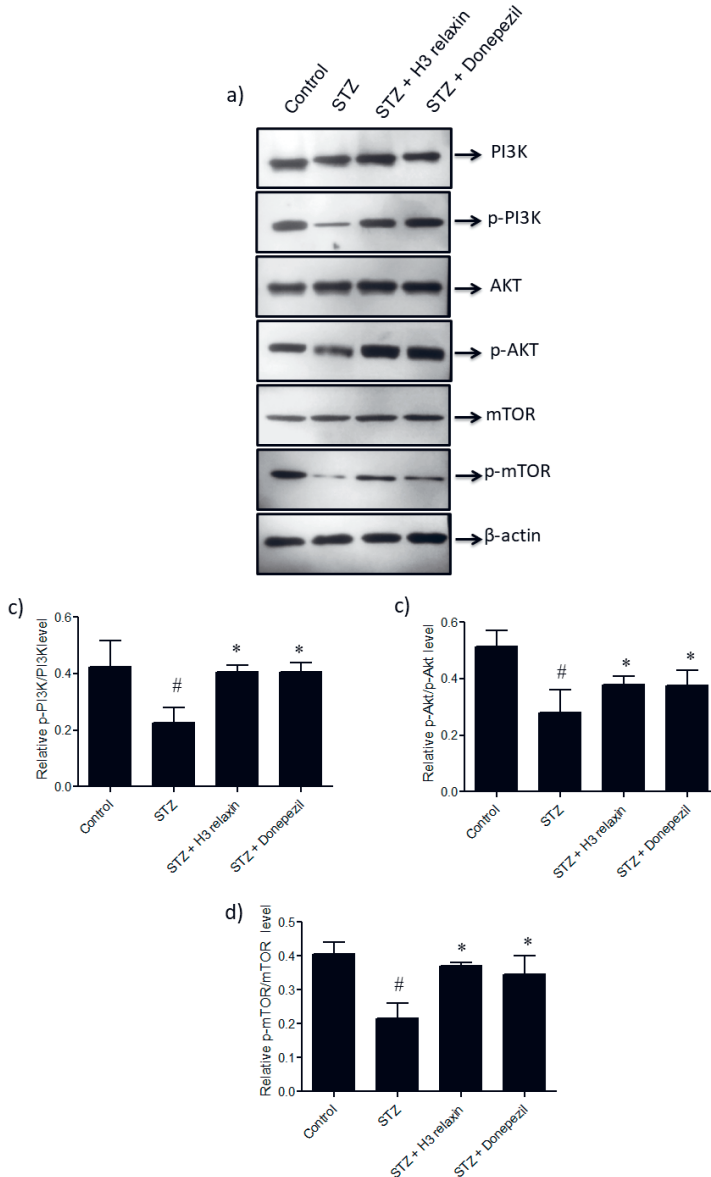


Fig. 5. Effects of H3 relaxin treatment on the PI3K/Akt/mTOR signalling pathway. a) Western blot analysis showing the expression and phosphorylation status of proteins involved within the PI3K/Akt/mTOR signalling pathway for each group of the experiment, portraying both phosphorylated and non-phosphorylated forms of PI3K, Akt, mTOR, and their upstream components; b), c) and d) represented ratio analysis of densitometric analysis for p-PI3K/PI3K, p-Akt/Akt, and p-mTOR/mTOR, respectively, were analysed quantitatively using ImageJ. Each experiment included biological replicates ( $n = 6$ ) and was performed in triplicate. # $p < 0.05$ , vs. control group, and \* $p < 0.05$ , vs. STZ group.

## CONCLUSIONS

This study demonstrates that H3 relaxin provides significant neuroprotective effects in a streptozotocin-induced murine model of Alzheimer's disease. By improving cognitive performance and reducing A $\beta$  and tau pathologies, H3 relaxin modulates the PI3K/Akt-mTOR signalling pathway, enhances autophagy activity, and attenuates oxidative stress and neuroinflammation. These results indicate that H3 relaxin may represent a potential therapeutic agent for disease modification in Alzheimer's. However, further studies are required to evaluate its long-term efficacy, optimal routes of administration, and translational feasibility for clinical use.

*Statement of ethics.* – The authors have no ethical conflicts to disclose.

*Acknowledgement.* – The authors would like to acknowledge the funding from the Ongoing Research Funding Program (ORF-2025-371), King Saud University, Riyadh, Saudi Arabia.

*Conflict of interest.* – The authors declare no conflict of interest.

*Author's contribution.* – Conceptualisation and study design, H.Z.; methodology, H.Z and Y. S.; statistical analysis, H.G.; writing, original draft preparation, S.A.H.; writing, review and editing, H.Z, Y.S., and H.G.; supervision, H.G. All authors have read and agreed to the published version of the manuscript.

## REFERENCES

1. P. T. Kamatham, R. Shukla, D. K. Khatri and L. K. Vora, Pathogenesis, diagnostics, and therapeutics for Alzheimer's disease: Breaking the memory barrier, *Ageing Res. Rev.* **101** (2024) Article ID 102481 (23 pages); <https://doi.org/10.1016/j.arr.2024.102481>
2. X. Xia, Q. Jiang, J. McDermott and J. J. Han, Aging and Alzheimer's disease: Comparison and associations from molecular to system level, *Aging Cell* **17**(5) (2018) e12802 (14 pages); <https://doi.org/10.1111/accel.12802>
3. Alzheimer's Association, 2024 Alzheimer's disease facts and figures, *Alzheimers Dement.* **20**(5) (2024) 3708–3821; <https://doi.org/10.1002/alz.13809>
4. A. A. Rostagno, Pathogenesis of Alzheimer's disease, *Int. J. Mol. Sci.* **24**(1) (2023) Article ID 107 (4 pages); <https://doi.org/10.3390/ijms24010107>
5. S. Tiwari, V. Atluri, A. Kaushik, A. Yndart and M. Nair, Alzheimer's disease: Pathogenesis, diagnostics, and therapeutics, *Int. J. Nanomed.* **14** (2019) 5541–5554; <https://doi.org/10.2147/IJN.S200490>
6. N. Guo, X. Wang, M. Xu, J. Bai, H. Yu and Z. Le, PI3K/AKT signaling pathway: Molecular mechanisms and therapeutic potential in depression, *Pharmacol. Res.* **206** (2024) Article ID 107300 (12 pages); <https://doi.org/10.1016/j.phrs.2024.107300>
7. J. Pan, Q. Yao, Y. Wang, S. Chang, C. Li, Y. Wu, J. Shen and R. Yang, The role of PI3K signaling pathway in Alzheimer's disease, *Front. Aging Neurosci.* **16** (2024) Article ID 1459025 (17 pages); <https://doi.org/10.3389/fnagi.2024.1459025>
8. S. Davoody, A. Asgari Taei, P. Khodabakhsh and L. Dargahi, mTOR signaling and Alzheimer's disease: What we know and where we are?, *CNS Neurosci. Ther.* **30**(4) (2024) e14463 (17 pages); <https://doi.org/10.1111/cns.14463>
9. W. Li, P. He, Y. Huang, Y. F. Li, J. Lu, M. Li, H. Kurihara, Z. Luo, T. Meng, M. Onishi, C. Ma, L. Jiang, Y. Hu, Q. Gong, D. Zhu, Y. Xu, R. Liu, L. Liu, C. Yi, Y. Zhu, N. Ma, K. Okamoto, Z. Xie, J. Liu, R. R. He and D. Feng, Selective autophagy of intracellular organelles: Recent research advances, *Theranostics* **11**(1) (2021) 222–256; <https://doi.org/10.7150/thno.49860>

10. Y. Zhao, Y. Zhang, J. Zhang, X. Zhang and G. Yang, Molecular mechanism of autophagy: Its role in the therapy of Alzheimer's disease, *Curr. Neuropharmacol.* **18**(8) (2020) 720–739; <https://doi.org/10.2174/1570159X18666200114163636>
11. M. Eshraghi, A. Adlimoghaddam, A. Mahmoodzadeh, F. Sharifzad, H. Yasavoli-Sharahi, S. Lorzadeh, B. C. Albensi and S. Ghavami, Alzheimer's disease pathogenesis: Role of autophagy and mitophagy focusing on microglia, *Int. J. Mol. Sci.* **22**(7) (2021) Article ID 3330 (36 pages); <https://doi.org/10.3390/ijms22073330>
12. Z. Zhang, X. Yang, Y. Q. Song and J. Tu, Autophagy in Alzheimer's disease pathogenesis: Therapeutic potential and future perspectives, *Ageing Res. Rev.* **72** (2021) Article ID 101464 (15 pages); <https://doi.org/10.1016/j.arr.2021.101464>
13. N. Mizushima, Autophagic flux measurement: Cargo degradation versus generation of degradation products, *Curr. Opin. Cell Biol.* **93** (2025) Article ID 102463 (8 pages); <https://doi.org/10.1016/j.ceb.2025.102463>
14. L. Gomez-Virgilio, M. D. Silva-Lucero, D. S. Flores-Morelos, J. Gallardo-Nieto, G. Lopez-Toledo, A. M. Abarca-Fernandez, A. E. Zacapala-Gomez, J. Luna-Munoz, F. Montiel-Sosa, L. O. Soto-Rojas, M. Pacheco-Herrero and M. D. Cardenas-Aguayo, Autophagy: A key regulator of homeostasis and disease – An overview of molecular mechanisms and modulators, *Cells* **11**(15) (2022) Article ID 2262 (40 pages); <https://doi.org/10.3390/cells11152262>
15. Z. Deng, Y. Dong, X. Zhou, J. H. Lu and Z. Yue, Pharmacological modulation of autophagy for Alzheimer's disease therapy: Opportunities and obstacles, *Acta Pharm. Sin. B* **12**(4) (2022) 1688–1706; <https://doi.org/10.1016/j.apsb.2021.12.009>
16. H. Leysen, D. Walter, L. Clauwaert, L. Hellemans, J. van Gastel, L. Vasudevan, B. Martin and S. Maudsley, The relaxin-3 receptor RXFP3 is a modulator of aging-related disease, *Int. J. Mol. Sci.* **23**(8) (2022) Article ID 4387 (22 pages); <https://doi.org/10.3390/ijms23084387>
17. S. Ma, C. M. Smith, A. Blasiak and A. L. Gundlach, Distribution, physiology and pharmacology of relaxin-3/RXFP3 systems in brain, *Br. J. Pharmacol.* **174**(10) (2017) 1034–1048; <https://doi.org/10.1111/bph.13659>
18. D. J. Scott, K. J. Rosengren and R. A. Bathgate, The different ligand-binding modes of relaxin family peptide receptors RXFP1 and RXFP2, *Mol. Endocrinol.* **26**(11) (2012) 1896–1906; <https://doi.org/10.1210/me.2012-1188>
19. J. R. Kumar, R. Rajkumar, T. Jayakody, S. Marwari, J. M. Hong, S. Ma, A. L. Gundlach, M. K. P. Lai and G. S. Dawe, Relaxin' the brain: Targeting the nucleus incertus network and relaxin-3/RXFP3 system in neuropsychiatric disorders, *Br. J. Pharmacol.* **174**(10) (2016) 1061–1076; <https://doi.org/10.1111/bph.13564>
20. M. E. S. Sorial, R. M. Abdelghany and N. El Sayed, Modulation of the cognitive impairment associated with Alzheimer's disease by valproic acid: Possible drug repurposing, *Inflammopharmacology* **33**(4) (2025) 2083–2094; <https://doi.org/10.1007/s10787-025-01695-0>
21. M. Levin-Arama, L. Abraham, T. Waner, A. Harmelin, D. M. Steinberg, T. Lahav and M. Harlev, Subcutaneous compared with intraperitoneal ketamine-xylazine for anesthesia of mice, *J. Am. Assoc. Lab. Anim. Sci.* **55**(6) (2016) 794–800.
22. D. Kaur, A. K. Grewal, S. H. Almasoudi, A. H. Almeahadi, B. A. Alsouk, A. Kumar, V. Singh, A. Alexiou, M. Papadakis, N. N. Welson, T. G. Singh and G. E.-S. Batiha, Neuroprotective effect of tozasertib in streptozotocin-induced Alzheimer's mice model, *Sci. Rep.* **15** (2025) Article ID 28963 (16 pages); <https://doi.org/10.1038/s41598-025-13920-5>
23. G. M. Shankar, M. A. Leissring, A. Adame, X. Sun, E. Spooner, E. Masliah, D. J. Selkoe, C. A. Lemere and D. M. Walsh, Biochemical and immunohistochemical analysis of an Alzheimer's disease mouse model reveals multiple cerebral amyloid- $\beta$  assembly forms, *Neurobiol. Dis.* **36**(2) (2009) 293–302; <https://doi.org/10.1016/j.nbd.2009.07.021>

24. L. J. Lissner, K. M. Wartchow, A. P. Toniazco, C. A. Goncalves and L. Rodrigues, Object recognition and Morris water maze to detect cognitive impairment from mild hippocampal damage in rats, *Pharmacol. Biochem. Behav.* **210** (2021) Article ID 173273 (9 pages); <https://doi.org/10.1016/j.pbb.2021.173273>
25. A. Vogel-Ciernia and M. A. Wood, Examining object location and object recognition memory in mice, *Curr. Protoc. Neurosci.* **69** (2014) 8.31.1-8.31.17; <https://doi.org/10.1002/0471142301.ns0831s69>
26. R. Rajmohan and P. H. Reddy, Amyloid- $\beta$  and phosphorylated tau accumulations cause synaptic abnormalities in Alzheimer's disease neurons, *J. Alzheimer's Dis.* **57**(4) (2017) 975–999; <https://doi.org/10.3233/JAD-160612>
27. H. Dong, C. M. Yuede, C. A. Coughlan, K. M. Murphy and J. G. Csernansky, Effects of donepezil on amyloid- $\beta$  and synapse density in the Tg2576 mouse model of Alzheimer's disease, *Brain Res.* **1303** (2009) 169–178; <https://doi.org/10.1016/j.brainres.2009.09.097>
28. K. Dasuri, L. Zhang, S. O. Kim, A. J. Bruce-Keller and J. N. Keller, Dietary and donepezil modulation of mammalian target of rapamycin signaling and neuroinflammation in the brain, *Biochim. Biophys. Acta Mol. Basis Dis.* **1862**(2) (2016) 274–283; <https://doi.org/10.1016/j.bbadis.2015.11.002>
29. S. Bathina and U. N. Das, Dysregulation of the PI3K-Akt-mTOR pathway in the brain of streptozotocin-induced type 2 diabetic rats, *Lipids Health Dis.* **17** (2018) Article ID 168 (11 pages); <https://doi.org/10.1186/s12944-018-0809-2>
30. Y. Fu, J. Zhang, R. Qin, Y. Ren, T. Zhou, B. Han and B. Liu, Activating autophagy to eliminate toxic protein aggregates in neurodegenerative diseases, *Pharmacol. Rev.* **77**(3) (2025) Article ID 100053 (50 pages); <https://doi.org/10.1016/j.pharmr.2025.100053>
31. Q. Wang, Y. Wang, S. Li and J. Shi, PACAP-sirtuin-3 alleviates cognitive impairment through autophagy in Alzheimer's disease, *Alzheimers Res. Ther.* **15**(1) (2023) Article ID 184 (20 pages); <https://doi.org/10.1186/s13195-023-01334-2>
32. S. Guo, L. Yi, M. Luo, Z. Dong and Y. Du, Parishin A ameliorates cognitive decline by promoting PS1 autophagy in Alzheimer's disease, *Front. Aging Neurosci.* **17** (2025) Article ID 1516190 (16 pages); <https://doi.org/10.3389/fnagi.2025.1516190>
33. F. Islam, M. H. Nafady, M. R. Islam, S. Saha, S. Rashid, S. Akter, M. H. Or-Rashid, M. F. Akhtar, A. Perveen, G. M. Ashraf, H. M. Rahman and S. H. Sweilam, Resveratrol and neuroprotection against Alzheimer's disease, *Mol. Neurobiol.* **59**(7) (2022) 4384–4404; <https://doi.org/10.1007/s12035-022-02859-7>
34. Y. Chen and Y. Yu, Tau and neuroinflammation in Alzheimer's disease: Interplay mechanisms and clinical translation, *J. Neuroinflammation* **20**(1) (2023) Article ID 165 (21 pages); <https://doi.org/10.1186/s12974-023-02853-3>
35. P. J. Ryan, E. Buchler, F. Shabanpoor, M. A. Hossain, J. D. Wade, A. J. Lawrence and A. L. Gundlach, Central RXFP3 activation decreases anxiety- and depressive-like behaviours in rats, *Behav. Brain Res.* **244** (2013) 142–151; <https://doi.org/10.1016/j.bbr.2013.01.034>
36. S. W. Jere, N. N. Hourelid and H. Abrahamse, Role of PI3K/AKT (mTOR and GSK-3 $\beta$ ) signaling in diabetic wound healing, *Cytokine Growth Factor Rev.* **50** (2019) 52–59; <https://doi.org/10.1016/j.cytogfr.2019.03.001>
37. C. Z. Yang, S. H. Wang, R. H. Zhang, J. H. Lin, Y. H. Tian, Y. Q. Yang, J. Liu and Y. X. Ma, Neuroprotective effect of astragaloside via activating PI3K/Akt-mTOR-mediated autophagy on APP/PS1 mice, *Cell Death Discov.* **9** (2023) Article ID 15 (13 pages); <https://doi.org/10.1038/s41420-023-01324-1>
38. S. A. El-Maraghy, A. Reda, R. M. Essam and M. A. Kortam, The citrus flavonoid "Nobiletin" impedes STZ-induced Alzheimer's disease in a mouse model through regulating autophagy mastered by SIRT1/FoxO3a mechanism, *Inflammopharmacology* **31**(5) (2023) 2701–2717; <https://doi.org/10.1007/s10787-023-01292-z>

39. Q. Qiu, X. Lei, Y. Wang, H. Xiong, Y. Xu, H. Sun, H. Xu and N. Zhang, Naringin protects against tau hyperphosphorylation via ER, PI3K/Akt and GSK-3 $\beta$  signaling, *Behav. Neurol.* **2023** (2023) Article ID 1857330 (16 pages); <https://doi.org/10.1155/2023/1857330>
40. M. A. Salem, B. Budzynska, J. Kowalczyk, N. S. El Sayed and S. M. Mansour, Tadalafil and bergapten mitigate STZ-induced sporadic Alzheimer's disease via PI3K/Akt, Wnt/ $\beta$ -catenin and AMPK/mTOR pathways, *Toxicol. Appl. Pharmacol.* **429** (2021) Article ID 115697 (14 pages); <https://doi.org/10.1016/j.taap.2021.115697>